

Passive thermography evaluation of bonding defects in adhered ceramic tiling: experimental and in-situ assessments

by J. Laranjeira*, N. Simões***, I. Simões*, A. Tadeu*** and C. Serra***

*CICC, Department of Civil Engineering, University of Coimbra, Pólo II, Rua Luís Reis Santos, 3030-788 Coimbra, Portugal, {nasimoes, joao.laranjeira, mivsimoes, tadeu, cserra}@itecons.uc.pt

**ITeCons - Instituto de Investigação e Desenvolvimento Tecnológico em Ciências da Construção, Rua Pedro Hispano, 3030-289 Coimbra, Portugal

Abstract

The paper deals with the application of passive thermography as a diagnostic tool to detect and evaluate bonding defects in adhered ceramic tiling. The bonding failure is a common building pathology and it represents serious risks to people's safety, particularly when it occurs in external cladding coating systems of tall buildings. In the first stage of this work, an evaluation of bonding defects was performed using both active and passive thermography techniques, by changing the type of heat source (i.e. artificial heat source versus sunlight). For this purpose, a set of test specimens with artificial defects inserted in the layer which adheres to the substrate were constructed (with varying sizes and placed at different depths) and were subjected to IR quantitative measurements by applying both techniques. After, several buildings with adhered ceramic cladding facades were selected to be qualitatively inspected through passive thermography. In order to accomplish this purpose, the specific environmental conditions that may allow bonding defects detection were assessed, particularly sky conditions (i.e. clear and cloudy sky) and the inspection time.

1. Introduction

Infrared (IR) thermography is a non-contact, fast and easy to apply technique, widely used for surface inspections of buildings and civil engineering structures ([1],[2]). This technique involves the use of an IR imaging instrument, an IR camera, to capture the energy emitted by the inspected surface materials or structures and their surroundings [3], as any object with a temperature higher than $-273,15\text{ }^{\circ}\text{C}$ or 0 K emits IR radiation ([2],[4],[5]). The higher the surface temperature of an object is, the more IR radiation it emits, since the quantity of energy leaving a surface as radiant heat is proportional to its emissivity and the fourth power of its absolute temperature [6], based on the Stefan-Boltzmann law. The emissivity of a surface varies between zero (perfect reflector, e.g. mirror) and one (perfect emitter, e.g. unreal black body) [6], depending on the surface temperature, the wavelength of radiation, the direction of radiation, and the surface characteristics, such as texture, roughness/polish, color, and dirt ([2],[4]). However, for most practical cases in IR thermography, temperature and wavelength dependencies are not relevant [4]. Also, only observation angles larger than 45° , with respect to the surface normal, show directional dependencies [4]. Therefore, most common building materials, with the exception of metals, have emissivity values over 0,8 [3], particularly, most materials used in building finishes processes, i.e. emissivity values range from 0,90 to 0,96 [7]. The IR radiation reflected by the surroundings of the inspected surface material or structure is also detected by the IR camera, depending mainly on the surrounding radiation [8] and on the surface characteristics of the inspected material or structure [5].

Since IR thermography is a non-contact technique, an object's radiation may be attenuated by the atmosphere before it is detected by the IR camera due to radiation absorption, scattering, emission and/or turbulence ([12],[13]). IR cameras generally perform in two different IR wavelength bands, such as middle wave ($2 - 5\text{ }\mu\text{m}$) and long wave ($8 - 15\text{ }\mu\text{m}$) [5]. In long wavelength range, the atmosphere is relatively transparent from about 8 to $13\text{ }\mu\text{m}$ (i.e. the atmosphere does not absorb radiation significantly) and the scattering phenomenon is weak (i.e. redistribution of the radiation into all directions with loss in the travelling direction from surface to IR camera, as a result of the presence of aerosol, such as water droplets, dust, and others) as the wavelength increases the transmittance improves [5]. For large distances between the inspected surface and the IR camera (i.e. distances over 10 m [3]) and when the temperature of the inspected object is close to the ambient air temperature, the atmosphere emits its own radiation [5]. Finally, turbulence that is caused by winds or convection transport effects and results in surface uneven cooling [6] is generally important for hundreds meters distance between the inspected surface and the IR camera, and for high sensitivity IR cameras [5].

The IR radiation detected by the IR camera is converted into an electrical signal, that generates a temperature map of the inspected surface, i.e. a thermal image or a thermogram, in which each level of energy is represented on a color scale or a grey scale ([4],[5],[7]). The resulting thermal image may allow the detection of internal defects (i.e. voids, pores, or delaminations) at a certain depth, depending on their thermal properties being different from their surrounding (i.e. thermal conductivity, specific heat capacity, and apparent density ([2],[4]) and on the temperature differences compared to ambient air temperature.

If a material or structure presents a natural temperature difference that is sufficiently strong to allow the evaluation of the thermal pattern displayed in the resulting thermal image, it won't be necessary to apply an additional heat flow to the object. This approach to IR thermography is called a passive thermography technique ([2],[4],[9]). On the other hand, active thermography involves a deliberate application of an artificial thermal stimulus on a surface to generate a temperature difference by heating or cooling ([4],[9]). In this study, the use of sun radiation to heat a surface is classified as passive thermography.

In building inspections using passive thermography the environmental conditions affect the transfer of energy and consequently IR images acquisition and interpretation. Temperature differences may be due to heating coming from the inside while the outer walls are cooled by the surrounding outside air [4], or due to heating from the outside (due to sun radiation) while the internal side of external walls are cooled by the surrounding air, depending on the season of the year and the orientation of the facade under inspection (i.e. solar heat gain regarding the inspection time of day). The environmental conditions that may affect IR images acquisition and interpretation are direct (and indirect [4]) sun radiation, wind (with a varying speed [4]), moisture (e.g. from rain), ambient air temperature and relative humidity ([3],[6],[7]). Moreover, cooling effects during the night may also affect IR images, particularly sky conditions, as clear sky strongly increased radiant losses compared to completely cloud covered sky [4]. Therefore, in order to perform a building inspection with enough surface temperature differences as a function of time that may allow the detection of internal defects, each IR thermography inspection using sun as the natural heating source may require specific environmental conditions [3]. Furthermore, the orientation of the building surface under inspection affects the intensity of sun radiation, and consequently the amount of solar heat gain and the inspection time of day [10].

In active thermography, there are various methods available to generate a transient thermal gradient that affects the surface temperature distribution as a function of time [4], i.e. for thermal stimulation ([2],[11]), as well as for data analysis to process the resulting raw thermal images [11].

In both approaches, IR camera performance parameters, along with the operator experience may also influence the success of IR measurements acquisition and interpretation.

The assessment of the temperatures map obtained in the resulting IR image may be either qualitative and/or quantitative. While in some applications the estimation of defective areas is enough (i.e. qualitative inspection), in other applications it is relevant to characterize defective areas and determine their size, shape, depth and/or their thermal properties (i.e. quantitative inspection) [11]. For a quantitative assessment, the target thermal emissivity should be estimated ([3],[12]), as the knowledge of their value is essential for accurate temperature measurements ([5],[6]). The measurement of the reflected temperature, i.e. the temperature of the energy incident upon and reflected from the inspected surface [13], should also be estimated for quantitative assessments [12], as it allows the compensation for the reflection coming from the surrounding objects. For qualitative assessments in buildings inspection, the ASTM C 1060 [14] recommends taking IR measurements from several angles, particularly perpendicular, if possible, and from two opposite oblique angles, in order to detect the presence of reflected radiation and avoid false interpretation of thermal images. Finally, particularly in the active approach, different data analysis methods to process the resulting raw thermal images can be used for qualitative or quantitative assessments [11].

Taking into account that IR thermography technique requires in-depth knowledge of the parameters involved in the IR measurements and great experience in results interpretation [3], there is a great potential for the use of IR thermography [2] in ceramic tiles systems inspection as it allows the evaluation of their integrity, regarding durability problems, such as cracking, efflorescence or detachment ([15],[16]). Adhesive failure and/or detachment of adhered ceramic tiling are common building pathologies [17] that may be caused, among other factors, due to poor adhesion of the ceramics tiles at the time of their application [16]. Hollow areas may be created inside the ceramic tile cladding systems, either between the adhesive layer and the ceramic tile and/or between the adhesive layer and the substrate. Taking into account that these durability problems represent serious risks to people's safety, preventive inspections should be performed.

Traditionally, passive thermography has been the main technique used for qualitative inspection of bonding integrity of adhered ceramic tiling [1], especially in middle or high-rise building inspections [10], due to the use of the sun as the natural heating source. Active thermography is a more reliable technique for quantitative inspections, since it has been proven that bonding defects can be observed and characterized, by using a controlled thermal load on the adhered ceramic tiling ([1],[16],[17],[18]).

Li et al. [16] applied both passive and active thermography techniques to the detection of bonding defects in adhered ceramic tiling and the results evidenced the reliability of both IR thermography techniques. Moreover, the authors proposed an effective approach to eliminate the disturbance of reflection in a building inspection, by suggesting the recording of IR images during the surface thermal stimulation period (by direct sun radiation) and when the clouds block the sun, since the effect of surface reflection is minimized and the temperature detected by IR camera correspond to the actual surface temperature. The IR images should be recording continuously the same area without moving the IR camera. Taking into account this approach, the authors propose a partially cloudy sky as a favourable weather condition.

Edis et al. [15] studied the factors that may affect IR measurements acquisition and interpretation by performing several building inspections of adhered ceramic claddings, generally, after sunset to avoid the intrusion of sunlight. Those factors were structured into an interaction matrix that distinguishes the relationship among them, and also their potential effects on IR thermography results. Based on the analysis of the interaction matrix, we may conclude that factors such as a building's shape (i.e. horizontal and vertical projections), facade orientation (i.e. amount of solar heat gain) and its surrounding elements (i.e. buildings, other structures, or trees standing in the path of sun exposure) are relevant due to uneven solar heat gains and reflection effects, which may produce false indications or may mask

problems. Surface characteristics such as texture, roughness, and dirt are also relevant, due to emissivity changes and reflection effects, as well as existing color patterns on the surface which lead to uneven solar heat gain.

Unsteady thermal conditions provided by either passive or active thermography are usually preferred for the detection of bonding defects filled with air [15]. A bonding defect area filled with air shows higher surface temperature in IR images than its surrounding area, during the heating period, while during the cooling period it shows lower surface temperature ([15],[16]). One the other hand, the detection of bonding defects filled with water through the application of passive thermography specifically requires unsteady thermal conditions [3]. There are two driving forces that generate thermal contrast in moist areas [15]: the use of evaporative cooling that leads to lower surface temperatures in moist areas [10] due to endothermic nature of evaporation [10], and the use of the increased specific heat capacity of moist materials that are either cooler or warmer than its surroundings, depending on it being the heating or cooling period [15], respectively, since specific heat capacity of water is higher than that of most construction materials [10].

Finally, Meola [19] reported that IR thermography technique is still not completely exploited and Edis et al. [15] mentioned that studies on bonding defects of ceramic tiling are still limited in number and usually consider active and/or quantitative thermography applications.

In this context, the first purpose of this paper is to apply and compare both active and passive thermography techniques to the detection and evaluation of bonding defects in adhered ceramic tiling with the different heat sources (i.e. artificial heat source versus sunlight). Taking into account the number and interaction of factors that may affect IR measurements acquisition and interpretation, firstly IR measurements were performed in the laboratory, and then, onsite, in building inspections. Then, a set of test specimens with artificial defects within the layer which adheres to the substrate (with varying sizes and depths) were constructed and subjected to IR quantitative measurements by applying both techniques. Several buildings with facades with adhered ceramic cladding were selected to be qualitatively inspected using passive thermography. In order to accomplish this purpose, the specific environmental conditions that may allow bonding defects detection were assessed, particularly the sky conditions (i.e. clear and cloudy sky) and the inspection time of day.

2. Experimental procedure

2.1. Laboratory measurements

For laboratory measurements, a set of test specimens of direct adhered ceramic tiles were prepared. Dense cement wood boards were used as a substrate with cementations adhesive mortar as the adhesive layer and ceramic tiles 9 mm thick as the final coating. The uncoated space of the substrate board was covered on both sides with expanded polystyrene foam (EPS), in order to decrease heat losses on the test specimens' boundaries.

Defects in the adhered layer were created between the adhesive layer and the ceramic tile and also between the adhesive layer and the substrate. The defects between the adhesive layer and the substrate were induced (e.g. extruded polystyrene foam (XPS)) with different sizes and depths. Defect depths were measured using an electronic caliper rule after the ceramic tiles were removed, after the infrared (IR) measurements.

Active and passive IR measurements were performed with an IR video camera (model A615 from FLIR Systems) and a computer system, in a controlled laboratory environment (23 ± 2 °C and 50 ± 5 %). The IR camera used has the following features: spectral range of 7,5-14 μm , field of view of $25^\circ \times 19^\circ$, spatial resolution of 0,68 mrad, focal length of 24,6 mm, IR detector with 640x480 pixels resolution, thermal sensitivity lower than 0,05 °C at 30 °C, an temperature accuracy of ± 2 °C or 2 %.

The active thermography measurements were performed using the software IR-NDT version 1.74 from Automation Technology. The specimens' surface stimulation was obtained using two halogen lamps (2500 W each), in reflection mode (i.e. thermal energy is delivered to the surface from the same side from which data is recorded). The experimental procedure adopted was a period of 120 s of heating performed with a rectangular modulated curve, 150 s of cooling, an acquisition frequency defined at 6,25 Hz, 100 % of the available heating power and data processing to obtain phase images and amplitude images.

In the passive thermography measurements, the test specimens were stimulated outside under direct sun radiation (i.e. clear sky conditions) between 9:30 a.m. to 15:30 p.m. (figure 1a) which was followed by a video recording of the cooling down process (of 240 s at an acquisition frequency of 6,25 Hz) in the laboratory using the software IRControl version 4.59 from Automation Technology (figure 1b). Passive IR measurements were performed in September, 2013, and the meteorological conditions during the heating period were measured by the Geophysical Institute of the University of Coimbra (IGUC).

In order to perform quantitative IR measurements, the reflected temperature and the target thermal emissivity were measured with the software IRControl version 4.59. The reflected temperature was estimated, based on [13], by placing a crumpled up piece of aluminium foil on the surface and measuring the average temperature of the foil target, with emissivity set to one. After adjusting the reflected temperature value, the target thermal emissivity was measured based on [20]. The thermal emissivity estimated for ceramic tiles with a black finishing color was 0,95. Before each IR measurement the measured parameters and the distance between the surface of the test specimen and the IR video camera, that was less than 1 m, were set in the corresponding software.

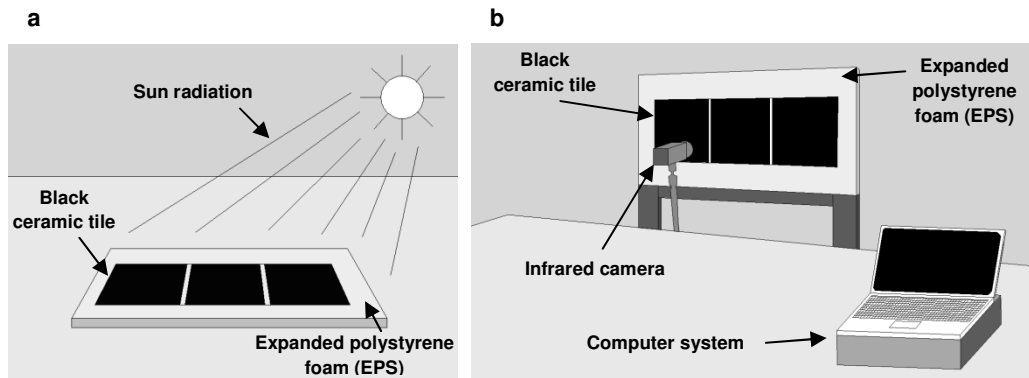


Fig. 1. Schematic drawing of the experimental set-up and sequence performed in passive infrared (IR) measurements: (a) 1st step - heating process of a test specimen outside under direct sun radiation; and (b) 2nd step - cooling down process of a test specimen inside the laboratory.

2.2. Building inspections

A number of buildings with facades of adhered ceramic cladding, located in Coimbra, Portugal, were qualitatively inspected using passive thermography, in order to detect adhesive failure and/or detachment of the adhered ceramic tiling. For each inspected facade, the infrared (IR) measurements were performed perpendicularly to the exterior wall surface and from two opposite oblique angles, whenever possible, in order to detect potential false indications that may result from radiation reflected from the surrounding objects.

As the sun was used as the natural heating source, sky conditions (i.e. clear and cloudy sky) and inspection time of day (considering facade orientation) were assessed. Passive IR inspections were performed between the months of March and May 2014, and the meteorological conditions during the inspection periods were measured by the Geophysical Institute of the University of Coimbra (IGUC). For cloudy sky conditions, completely or partially cloudy sky was considered.

The IR measurements in building inspections were performed with an IR camera (model ThermaCAMTM T360 from FLIR Systems) that allows the obtaining of IR and visual images simultaneously. The values of the parameters of the IR camera used are the following: spectral range of 7,5-13 μm , field of view of 25°x18,75°, spatial resolution of 1,36 mrad, focal length of 18,04 mm, IR detector with 320x240 pixels resolution, thermal sensitivity lower than 0,08 °C at 30°C, and a temperature accuracy of ± 2 °C or 2 %.

3. Discussion of results

3.1. Laboratory measurements

Figures 2b, c and d show the thermal response of the test specimen surface with the extruded polystyrene (XPS) defects obtained using the active thermography technique, while figure 2e shows the thermal response using a passive approach. Considering the schematic drawing in figure 2a, the majority of the induced defects (i.e. defects with a thickness of 3 to 4 mm between the adhesive layer and the substrate placed at an average depth of 2,3 mm for the rectangular defect and 1,9 mm and 2,4 mm for the squared figures (left and right, respectively)) are visible on the infrared (IR) images as shown by the contrasts achieved between defect and non-defect areas. However, additionally, non-induced defects are also detectable. After the ceramic tile was removed (figure 2f) the existence of air gaps between the adhesive layer and the ceramic tile with thicknesses of less than 1 mm was discovered, corresponding to the non-induced defects visible on the IR images.

During the heating process, the heat flow applied on the test specimen surface resulted from halogen lamps (for active approach) and sunlight exposure (for passive approach). The presence of the induced defects (i.e. XPS) and the non-induced ones (i.e. air gaps) interferes with the heat flow since defects act as a barrier for heat propagation and surface temperature distribution on defected areas is modified. It should be noted that the thermal image (figure 2b) from the active approach shows defect areas with a lighter color (corresponding to high temperatures, for a grey scale), while the thermal image (figure 2e) that resulted from using the passive approach shows defect areas with a darker color (corresponding to lower temperatures). Both images (figure 2b and e) resulted from the cooling down process. Indeed, the analysis of the isotherm line (2) in figure 2e and the corresponding surface temperatures graphic (2) reveal a significant surface temperature variation on the XPS defect areas (i.e. both square figures) and on the non-induced air gap in the lower right corner of the thermal image. This change in surface temperature patterns may result from the fact that, in the passive approach, the heating process occurred for a longer time, allowing the storage of thermal energy on the areas with more mass available, which are the zones without defects. Moreover, it is visible that defect detectability in the thermal image from the passive approach is much better than the thermal image from the active approach.

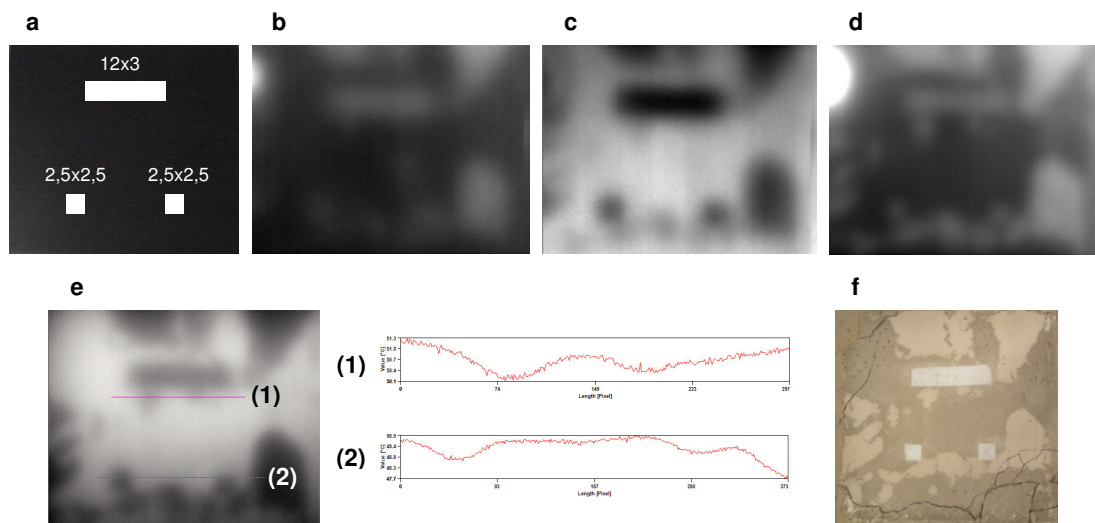


Fig. 2. Test specimen with the extruded polystyrene (XPS) defects: a) schematic drawing (area defects in cm^2); b) raw thermal image from active approach; c) phase image obtained with pulse phase evaluation algorithm from active approach; d) amplitude image obtained with Lock-in harmonic approximation algorithm from active approach; e) thermal image from passive approach and surface temperature graphics from isotherm lines (1,2); and f) photo after the black ceramic tile has been removed.

(Infrared images with (b) a temperature scale ($^{\circ}\text{C}$) of 27,6 – black to 34,1 – white; (c) a phase scale of -1,824 - black to -0,701 – white; (d) an amplitude scale of 69,23 - black to 400,11 – white; and (e) a surface temperature scale ($^{\circ}\text{C}$) of 47,1 – black to 51,7 - white)

(Environmental conditions during the heating period with clear sky of the test specimen at September 20, 2013 (average values): ambient air temperature of 28,1 $^{\circ}\text{C}$, relative humidity of 45,2 %, wind speed of 0,8 m/s)

Phase and amplitude images (figures 2c and d, respectively) resulted from the application of signal processing algorithms to raw thermal images (figure 2b) and it is visible that defect detectability was clearly improved. The phase image (figure 2c), that resulted from the application of the *pulse phase evaluation algorithm*, shows better contrasts between defect and non-defect area, then the amplitude image (figure 2d), that resulted from the application of the *Lock-in harmonic approximation algorithm*.

An analysis of some of the non-induced defects reveals that the air gaps immediately below the rectangular figure observed in figure 2f are more visible in the amplitude image than in the phase image. In the thermal image from the passive approach (figure 2e) those air gaps are also detected, as well as in the surface temperature graphic of isotherm line (1), where a significant surface temperature variation is shown on the defect areas.

3.2. Building inspections

Building A

Figure 3 presents some photos and infrared (IR) images of a building facade with an unglazed ceramic tile cladding, facing West (building A), and without surrounding buildings nearby. Based on figure 3a, an adhesive failure and detachment of the adhered ceramic tiling (highlighted with a rectangle) is detectable. In IR images, the bonding defect is seen in the heating and cooling down periods (figures 3b and c, respectively), by showing a higher and lower surface temperature, respectively, than their surroundings. In IR image 3c, which resulted from the inspection performed during a cold period, the structural elements (i.e. columns and slab cross section) on the masonry are visible, which did not happened in IR image 3b (inspection performed during heating period).

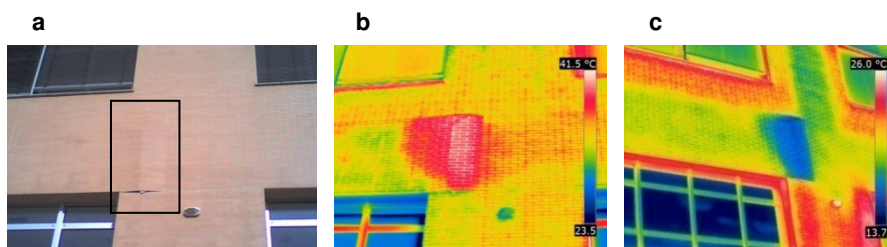


Fig. 3. West facade of building A: a) photo of facade under direct sun radiation on April 8, 2014, b) thermal image of the surface under sun radiation from inspection performed with clear sky, that started at 4:00 p.m.; and c) thermal image of the surface from inspection performed with clear sky, that started at 8:30 p.m..

(Environmental conditions during inspection on April 8, 2014: (b) ambient air temperature of 25,5 $^{\circ}\text{C}$, relative humidity of 57,7 %, wind speed of 1,9 m/s; and (c) 18,2 $^{\circ}\text{C}$, 79,8 %, 2,2 m/s)

Building B

In another building inspection (Building B), a different thermal pattern (highlighted with a circle) is detected on the ceramic tile cladding, that is shown on the three IR images obtained with a perpendicular angle (figure 4b) and two opposite oblique angles (figures 4c and d) to building facade. Taking into account that the inspection on the building South-East facade was performed during the heating period (i.e. at 1:30 p.m. with clear sky), the suspicious area presents higher surface temperature than their ceramic tile surrounding on IR images. This thermal pattern may be caused by a bonding defect, however, according to figure 4a, the suspicious area does not present pathological evidences on their surface that may indicate the presence of a bonding defect. Other suspicious thermal patterns are also detected on the ceramic tile cladding. Therefore, in order to learn the thermal patterns behaviour of the possible bonding defects identified in figure 4, aimed at confirming the existence of bonding defects, more inspections were performed at several other times of day and with clear and cloudy sky conditions. Table 1 presents a set of IR image of each inspection performed to that particular area of the building B.

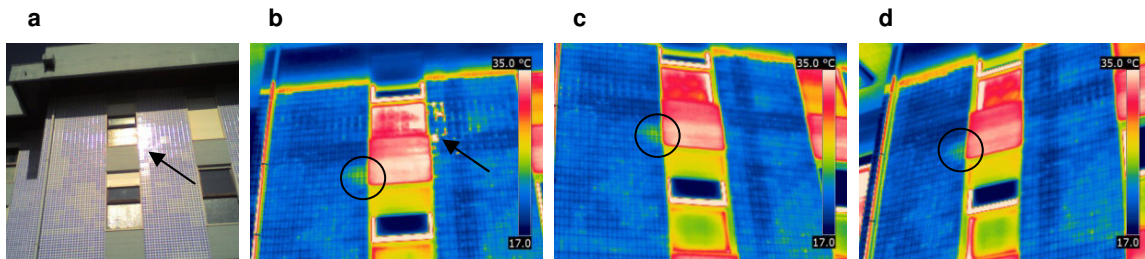


Fig. 4. South-East facade of building B: a) photo of the facade under direct sun radiation; b) thermal image of the surface from a perpendicular angle; c) thermal image of the surface from an oblique angle; and d) thermal image of the surface from the opposite oblique angle.

(Environmental conditions during inspection with clear sky at March 15, 2014, that started at 1:30 p.m.: ambient air temperature of 20,9 °C, relative humidity of 51,5 %, wind speed of 1,6 m/s)

The thermal pattern highlighted with a circle on figure 4 (inspection started at 1:30 p.m.) are also detected earlier, at 10:00 a.m., during clear sky (different inspection days), both with higher surface temperature than the ceramic tile surrounding, as inspections were performed during heating period (building B in table 1). At 3:45 p.m., the thermal pattern is not detected when the building facade was already in the shadow of the nearby building (i.e. cooling period). Inspections performed at 7:30 p.m. and 9:00 p.m. evidence the thermal pattern, but showed a lower surface temperature (i.e. the cooling period continuous).

During cloudy sky conditions, the suspicious thermal pattern shows the same behaviour. Firstly, during the heating period, it shows a higher surface temperature, while during cooling period, it shows a lower surface temperature than their ceramic tile surrounding (building B in table 1). At 9:30 a.m., the suspicious thermal pattern is not detected, probably as a result of the completely cloudy sky conditions and the inspection time of day (at 9:30 a.m. the ambient air temperature was the lowest one of the inspections days with cloudy sky), considering facade orientation (building B in table 1).

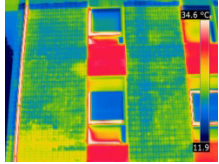
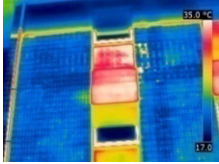
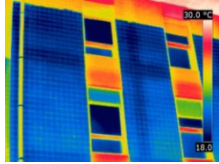
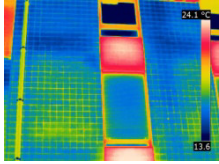
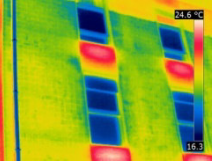
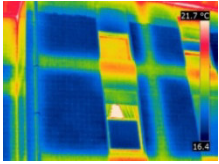
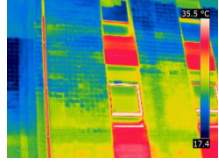
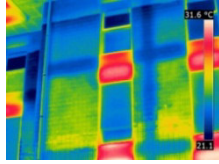
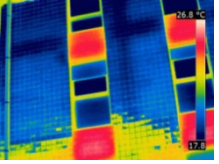
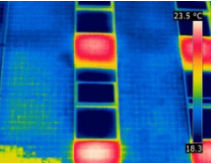
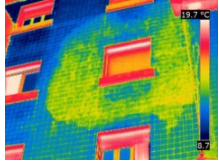

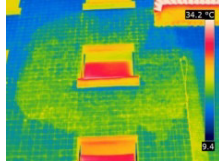

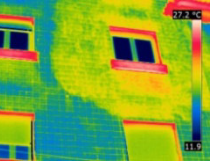
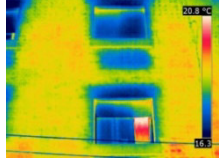
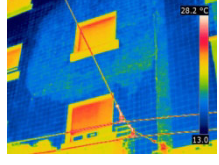

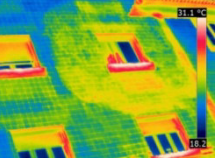

Therefore, this analysis reveals that it is quite possible that that area has a bonding defect filled with air. Confirmation could be achieved by performing a repercussion test that would require building a temporary structure, as this corresponds to a facade area between the second and the third floor.

In figure 4b (obtained from a perpendicular angle) visible some spots on the ceramic tile cladding with the higher surface temperature (i.e. the maximum of surface temperature scale) are pointed out. That area is also pointed out in figure 4a and it shows sunlight reflection, due to the perpendicular angle and glazed surfaces. Indeed, both images (figures 4a and b) resulted from the same perpendicular angle. However, in the IR image obtained, on another inspection, taken also from a perpendicular angle and during a heating period, but at 10:00 a.m. (building B in table 1) the sunlight reflection is not detected. This is probably due to a difference in sun direction, considering the different time of day.

The ceramic tile cladding shows changes in surface color patterns (figure 4a), the majority of which are also identified on IR images obtained from some inspections (figures 4b, c and d, and building B in table 1). Building users shared that a partial renewal of tiles had been performed in the past, which probably justify these thermal pattern changes. It is interesting to note that, the changes in surface color patterns of the ceramic tiles cladding are visible under direct sun radiation.

Finally, the structural elements (i.e. beams and columns) are detected, but not on all IR images. They show lower surface temperatures on the ceramic tile cladding, except at 9:30 a.m. with completely cloudy sky (i.e. before heating period) (building B in table 1). The shadow caused by the horizontal overhang on ceramic tile surface is also detected in some of the IR images, with lower and higher surface temperature, depending on the time of day and sky conditions.

Table 1. Some building inspection results with passive thermography technique with clear and cloudy sky conditions and at several time of day.

Building B South-East facade	Clear sky					
	Inspection starting time and date	10:00 a.m., April 29, 2014	1:30 p.m., March 15, 2014	3:45 p.m., May 8, 2014	7:30 p.m., April 8, 2014	9:00 p.m., April 10, 2014
	Environmental conditions⁽¹⁾	16,8 °C/68,7 %/1,4 m/s	21,6 °C/47,9 %/1,5 m/s	22,3 °C/59,1 %/4,7 m/s	19,1 °C/76,3 %/2,7 m/s	IGUC equipment problem
	Effect of sun radiation and/or shadows	Under direct sun radiation	Under direct sun radiation	Under nearby building shadow	Under nearby building shadow	-
	Cloudy sky					
	Inspection starting time and date	9:30 a.m., May 6, 2014	12:30 a.m., April 30, 2014	2:30 p.m., April 28, 2014	6:15 p.m., April 30, 2014	8:00 p.m., April 22, 2014
	Environmental conditions⁽¹⁾	15,5 °C/84,5 %/1,8 m/s	21,5 °C/69,4 %/1,5 m/s	20,1 °C/67,2 %/2,6 m/s	18,8 °C/79,9 %/4,7 m/s	16,0 °C/69,4 %/1,6 m/s
Effect of sun radiation and/or shadows	Under indirect sun radiation ⁽²⁾	Under direct and indirect sun radiation ⁽³⁾	Under direct and indirect sun radiation ⁽³⁾	Under nearby building shadow ⁽³⁾	Under nearby building shadow ⁽³⁾	
Building C South-West facade	Clear sky					
	Inspection starting time and date	9:15 a.m., April 29, 2014	11:15 a.m., April 8, 2014	2:10 p.m., May 13, 2014	7:00 p.m., April 10, 2014	8:15 p.m., April 8, 2014
	Environmental conditions⁽¹⁾	15,4 °C/72,7 %/1,4 m/s	19,0 °C/81,4 %/0,6 m/s	25,3 °C/ 40,2 %/ 3,4 m/s	IGUC equipment problem	18,2 °C/79,8 %/2,2 m/s
	Effect of sun radiation and/or shadows	Under their shadow	Under their shadow	Under direct sun radiation	Under nearby building shadow	Under nearby building shadow
	Cloudy sky					
	Inspection starting time and date	8:00 a.m., April 18, 2014	11:45 a.m., April 30, 2014	2:15 p.m., April 29, 2014	5:45 p.m., April 30, 2014	7:30 p.m., April 22, 2014
	Environmental conditions⁽¹⁾	13,8 °C/100,0 %/0,4 m/s	20,0 °C/74,9 %/0,8 m/s	21,8 °C/64,4 %/3,3 m/s	19,8 °C/77,3 %/4,6 m/s	16,6 °C/68,5 %/2,0 m/s
Effect of sun radiation and/or shadows	Under their shadow ⁽²⁾	Under their shadow ⁽³⁾	Under direct and indirect sun radiation ⁽³⁾	Under direct and indirect sun radiation ⁽³⁾	Under nearby building shadow ⁽³⁾	

⁽¹⁾Ambient air temperature (°C)/ relative humidity (%) / wind speed (m/s)

⁽²⁾Completely cloudy sky

⁽³⁾Partially cloudy sky

Building C

In a first inspection on the South-West facade of building C, a suspicious thermal pattern that may be the result of a bonding defect was found around a second floor window, in two of the three IR images obtained with different observation angles (figures 5b and d). The analysis of figure 5a does not reveal any superficial pathology that may be responsible for these thermal patterns behaviour. Furthermore, the building in front of the facade area under inspection is coated with a non-reflective yellow paint over a mortar layer. The inspection of this suspicious area of the building facade, performed at several times, and under clear and cloudy sky conditions (building C in table 1), demonstrated that the same thermal pattern is detected in the IR images, except for the IR images that resulted from 8:00 a.m. inspection with completely cloudy sky (i.e. before heating period). Furthermore, when detected, the thermal pattern always presented a higher surface temperature than that of the glazed ceramic tile surrounding, which may be due to a bonding defect.

Taking into account that the thermal pattern around that second floor window was detected with other inspection conditions (building C in table 1), in particular with similar observation angles as in figure 5c, the change of the thermal pattern around that second floor window with the observation angle (figure 5c) may be due to parked cars on the sloping and narrow street, as cars may reflect sunlight on glazed ceramic tile facades. Furthermore, the partially cloudy sky could also be responsible for that thermal pattern changes with the observation angle.

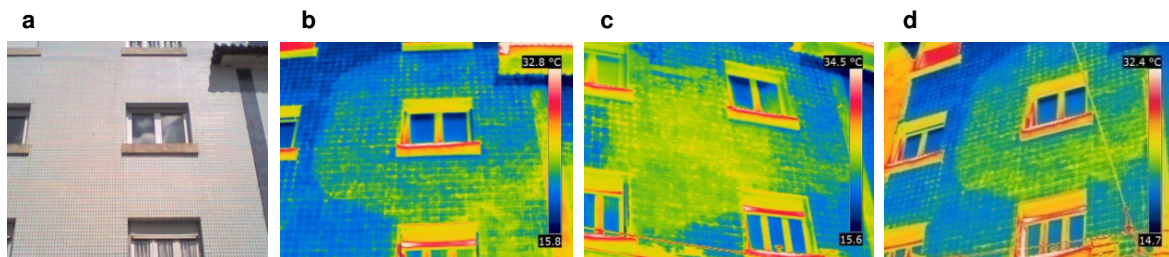


Fig. 5. South-West facade of building C: a) photo of the facade under direct and indirect sun radiation; b) thermal image of the surface from a perpendicular angle; c) thermal image of the surface from an oblique angle; and d) thermal image of the surface from the opposite oblique angle.

(Environmental conditions during inspection with partially cloudy sky at April 29, 2014, that started at 2:15 p.m.: ambient air temperature of 21,8 °C, relative humidity of 64,4 %, wind speed of 3,3 m/s)

Building D

South-West facade inspections of building D evidence several areas of the ceramic tile cladding with a lower surface temperature (IR images in figure 6). These thermal patterns may be the result of heterogeneous areas in the support and not of bonding defects, since the inspection of this building facade area at several time of day and with clear and cloudy sky conditions, revealed that the suspicious areas were always detected with lower surface temperature than the ceramic tile surrounding. Moreover, at the beginning of the heating period with completely cloudy sky, the suspicious areas were less detectable. Additionally, the building facade does not show evidence of any superficial pathology (figure 6a).

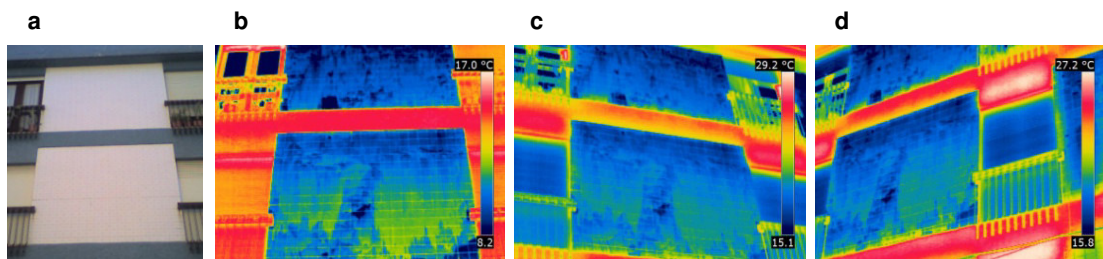


Fig. 6. South-West facade of building D: a) photo of facade under their shadow; b) thermal image of the surface from a perpendicular angle (facade under their shadow); c) thermal image of the surface from an oblique angle (facade under direct sun radiation); and d) thermal image of the surface from the opposite oblique angle (facade under nearby building shadow).

(Environmental conditions during inspection with clear sky (b) at April 29, 2014, that started at 9:15 a.m.: ambient air temperature of 15,4 °C, relative humidity of 72,7 %, wind speed of 1,4 m/s; (c) at May 8, 2014, that started at 4:00 p.m.: 22,3 °C, 62,2 %, 4,5 m/s; and (d) at May 8, 2014, that started at 8:00 p.m.: 16,2 °C, 86,6 %, 3,3 m/s)

Building E

Figure 7 presents a particular case of a re-entrant corner inspection on the building E (South-West and North-West facades). Based on figure 7a three areas of adhesive failure of the adhered ceramic tiling are detectable. Those bonding defect areas are also visible on the IR images of figure 7. Moreover, along with them, a thermal path with lower surface temperatures connecting two adhesive failure areas (those located on underside of the facade) and

another path crossing the other adhesive failure area (at the top of the facade) are visible. Based on the fact that no building facade cracking was found on that area (figure 7a), probably those thermal paths are the result of bonding defects in the ceramic tile cladding. Furthermore, other areas of the ceramic tile cladding show higher surface temperatures, indicating that bonding defects may be gradually occurring.

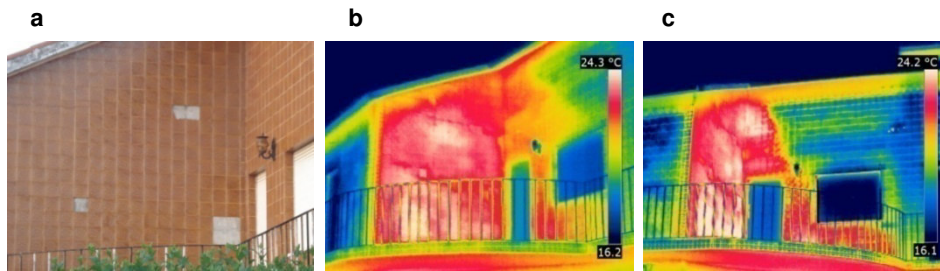


Fig. 7. South-West and North-West facades of Building E: a) photo with three areas of adhesive failure of the adhered ceramic tiling on a re-entrant corner; b) thermal image of the re-entrant corner from inspection performed with clear sky, at April 10, 2014, that started at 10:00 p.m.; and c) thermal image of the re-entrant corner from inspection performed with partially cloudy sky at April 22, 2014, that started at 10:00 p.m..

(Environmental conditions during inspection: (b) IGUC equipment problem; and (c) ambient air temperature of 14,3 °C, relative humidity of 79,5 %, wind speed of 1,4 m/s)

4. Conclusions

This paper deals with the application of both active and passive thermography techniques to the detection and evaluation of bonding defects in adhered ceramic tiling by comparing both techniques (i.e. artificial heat source versus sunlight). Taking into account the number and interaction of factors that may affect infrared (IR) measurements acquisition and interpretation, firstly, IR quantitative measurements were performed in the laboratory, on a set of test specimens with artificial defects within the layer which adheres to the substrate, by applying both techniques. The purpose was to demonstrate the possibility of defect detection using the sun heating. Then, several buildings with facades of adhered ceramic cladding were qualitatively inspected using passive thermography (i.e. using the sun as the natural heat source) at different inspection times of day and under different environmental conditions (i.e. clear and cloudy sky).

Laboratory tests allowed the detection and evaluation of air gaps with thicknesses of less than 1 mm located at 9 mm depth from the ceramic tile surface, as well as of defects between the adhesive layer and the substrate, e.g. extruded polystyrene (XPS) defects with 2,5x2,5 cm², with a thickness of 3 to 4 mm, placed at a depth about 11,5 mm from the surface. Based on the experimental procedure performed, these tests demonstrate that bonding defect detectability on ceramic tile systems is not affected by the heat source change from halogen lamps to sunlight, when phase and/or amplitude images from active approach are compared with thermal images from passive approach.

Building inspections using a passive thermography technique evidence that, in some situations it may be useful to perform several inspections at different times of day, taking into account facade orientation, in order to confirm eventual defects through their thermal behavior along the daytime, as well as to avoid false interpretation of thermal images by performing IR measurements from several observation angles. This seems particularly pertinent on the inspection of glazed ceramic tile claddings, where reflections from nearby buildings, trees, cars may strongly affect temperature patterns. In this context, an adequate analysis of the surrounding environment should be performed.

Generally, bonding defects were detected with clear and cloudy sky conditions, particularly during or after the heating period, considering building facade orientation. Indeed, the inspections performed at the beginning of the heating period with cloudy sky did not allow bonding defect detection, particularly with completely cloudy sky, considering facade orientation. Moreover, inspections performed with partially cloudy sky conditions seem to affect the thermal patterns displayed on IR images introducing limitation to IR thermography use.

Acknowledgements

The research work presented herein was supported by FEDER funds through the Operational Programme for Competitiveness Factors - Compete and by national funds through the FCT – Portuguese Foundation for Science and Technology, under research project PTDC/ECM/114189/2009 and was supported in part by QREN - Compete under the research project Active Floor Project (FCOMP-01-0202-FEDER-021583. This work has also been supported by the Energy and Mobility for Sustainable Regions - EMSURE - Project (CENTRO-07-0224-FEDER-002004).

The authors acknowledge to Geophysical Institute of the University of Coimbra (IGUC) for providing climate data.

REFERENCES

- [1] Hung Y. Y., Chen Y. S., Ng S. P., Liu I., Huang Y. H., Luk B. L., Ip R. W. L., Wu C. M. L., Chung P. S., "Review and comparison of shearography and active thermography for nondestructive evaluation". *Materials Science and Engineering R*, vol. 64, pp. 73-112, 2009.
- [2] Maldague X., "Theory and practice of infrared technology for non-destructive testing", pp. 1-618, John Wiley & Sons, 2001.
- [3] Freitas S. S., Freitas V. P., Barreira, E., "Application of infrared thermography to the diagnosis of façade rendering detachment" in Freitas V. P. ed. – "A state-of-the-art report on building pathology", Ch. 3.10 (e-book), CIB Publication 369, CIB – W086 Building Pathology, 2013.
- [4] Vollmer M., Mollmann K.-P., "Infrared thermal imaging. Fundamentals research and applications", pp. 1-593, Wiley-VCH Verlag GmbH & Co. KGaA, 2010
- [5] Meola C., "Origin and theory of infrared thermography" in Meola C. - "Infrared thermography recent advances and future trends", pp. 3-28, Bentham Science Publishers, 2012.
- [6] Balaras C. A., Argiriou A. A., "Infrared thermography for building diagnostics". *Energy and Buildings*, vol. 34, pp. 171-183, 2002.
- [7] Plesu R., Teodoriu G., Tăranu G., "Infrared thermography applications for building investigation". *Universitatea Tehnică Gheorghe Asachi din Iasi. Tomul L VIII (LXII)(1), Constructii. Arhitectură*, 2012.
- [8] Marinetti S., Cesaratto P. G., "Emissivity estimation for accurate quantitative thermography". *NDT&E International*, vol. 51, pp. 127-134, 2012.
- [9] Cannas B., Carcangiu S., Concu G., Trulli N., "Modeling of active infrared thermography for defect detection in concrete structures", COMSOL Conference, Milan (Italy), 2012.
- [10] Edis E., Flores-Colen I., de Brito J., "Effect of the inspection conditions on the in-situ infrared thermographic examination of facades with adhered ceramic cladding". *XII Durability of Building Materials and Components, Porto (Portugal)*, 2011.
- [11] Ibarra-Castanedo C., Tarpani J. R., Maldague X. P. V., "Nondestructive testing with thermography". *European Journal of Physics*, vol. 34, pp. S91-S109, 2013.
- [12] Ciocia C., Marinetti S., "In-situ emissivity measurement of construction materials", *Proceedings of 11th Quantitative Infrared Thermography conference, paper QIRT2012-168, Naples (Italy)*, 2012.
- [13] ASTM E 1862-97, "Standard test methods for measuring and compensating for reflected temperature using infrared imaging radiometers". *American Society for Testing and Materials, Pennsylvania (USA)*, 2002.
- [14] ASTM C 1060-90, "Standard practice for thermographic inspection of insulation installations in envelope cavities of frame buildings". *American Society for Testing and Materials, Pennsylvania (USA)*, 2003.
- [15] Edis E., Flores-Colen I., de Brito J., "Passive thermographic inspection of adhered ceramic claddings: limitation and conditioning factors". *Journal of Performance of Constructed Facilities*, vol. 27(6), pp.737-747, 2013.
- [16] Li Z., Yao W., Lee S., Lee C., Yang Z., "Application of infrared thermography technique in building finish evaluation". *Journal of Nondestructive Evaluation*, vol. 19(1), pp. 11-19, 2000.
- [17] Simões N., Simões I., Tadeu A., Serra C., "Evaluation of adhesive bonding of ceramic tiles using active thermography", *Proceedings of 11th Quantitative InfraRed Thermography conference, paper QIRT2012-362, Naples (Italy)*, 2012.
- [18] Sfarra S., Ibarra-Castanedo C., Lambiase F., Paoletti D., Di Ilio A., Maldague X., "From the experimental simulation to integrated non-destructive analysis by means of optical and infrared techniques: results compared". *Measurement Science and Technology*, vol. 23, pp. 14, 2012.
- [19] Meola C., "A new approach for estimation of defects detection with infrared thermography". *Materials Letters*, vol. 61(3), pp. 747-750, 2007.
- [20] ASTM E 1933-99a, "Standard test methods for measuring and compensating for emissivity using infrared imaging radiometers". *American Society for Testing and Materials, Pennsylvania (USA)*, 2010.